Nanolayered siRNA Dressing for Sustained Localized Knockdown

Steven Castleberry,[†,‡] Mary Wang,[‡,§] and Paula T. Hammond[‡,§,*]

[†]Harvard-MIT Division of Health Sciences and Technology, Massachusetts Institute of Technology, Cambridge, Massachusetts 02139, United States , [‡]Department of Chemical Engineering, Massachusetts Institute of Technology, Cambridge, Massachusetts 02139, United States , and [§]David H. Koch Institute for Integrative Cancer Research at MIT, Cambridge, Massachusetts 02139, United States

ABSTRACT The success of RNA interference (RNAi) in medicine relies on the development of technology capable of successfully delivering it to tissues of interest. Significant research has focused on the difficult task of systemic delivery of RNAi; however its local delivery could be a more easily realized approach. Localized delivery is of particular interest for many medical applications, including the treatment of localized diseases, the modulation of cellular response to implants or tissue engineering constructs, and the management of wound healing and regenerative medicine. In this work we present an ultrathin electrostatically assembled coating for localized and sustained delivery of short interfering RNA (siRNA). This film was applied to a commercially available woven nylon dressing commonly used for surgical applications and was demonstrated to sustain significant knockdown of protein expression in multiple cell types for more than one week *in vitro*. Significantly, this coating can be easily applied to a medically relevant device and requires no externally delivered transfection agents for effective delivery of siRNA. These results present promising opportunities for the localized administration of RNAi.

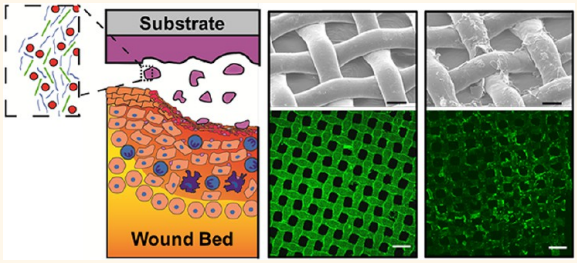

KEYWORDS: siRNA delivery · layer-by-layer (LbL) · controlled release · nanofilm · local delivery · polyelectrolyte multilayer · electrostatic assembly · tissue engineering

RNA interference (RNAi) holds enormous potential both as a tool in molecular biology and as a powerful therapeutic agent.[1−6] Currently however there remain significant questions as to the viability of RNAi in medicine due to the difficulty in delivering the molecule effectively to areas of interest while maintaining its activity and avoiding toxicity.[7−10] Whether advances in the systemic delivery of short interfering RNA (siRNA)[11−17] can effectively address these concerns is yet to be seen; technologies for the local administration of RNAi may offer more easily realized opportunities.[18−23] Local delivery can limit numerous unwanted systemic side effects of therapies and maintains the highest load possible in the targeted area before clearance.[24,25] The direct release of siRNA to certain regions of the body could be of significant interest in many applications: modifying cellular interactions with medical implants such as orthopedic implants and vascular stents, altering how cells respond to tissue engineering constructs, or serving as a localized reservoir for sustained therapeutic benefit. To the best of our knowledge, there have been relatively few attempts to develop material systems for localized and sustained delivery of siRNA to tissues.[22,26−28]

Layer-by-layer (LbL) assembly is a robust method that has been successfully demonstrated for the localized and sustained delivery of many biologic therapeutics and biomolecules.[29−32] LbL is the sequential adsorption of materials onto a surface using electrostatic, hydrogen bonding, or other complementary interactions.[33,34] Materials of interest can be uniformly coated on a surface with alternating interactions to generate nanometer-scale thin films that can deliver small-molecule drugs,[35] growth factors,[36] and DNA.[37] LbL films have been used to coat many different surfaces ranging from stainless steel[38] and titanium[39] to synthetic and naturally derived polymer constructs and even coating living organisms.[40] In addition, the delivery of siRNA from an LbL film could provide a platform for future applications where sequential and coordinated release[41,42] of siRNA along

* Address correspondence to hammond@mit.edu.

Received for review February 27, 2013 and accepted May 14, 2013.

Published online May 14, 2013
10.1021/nn401011n

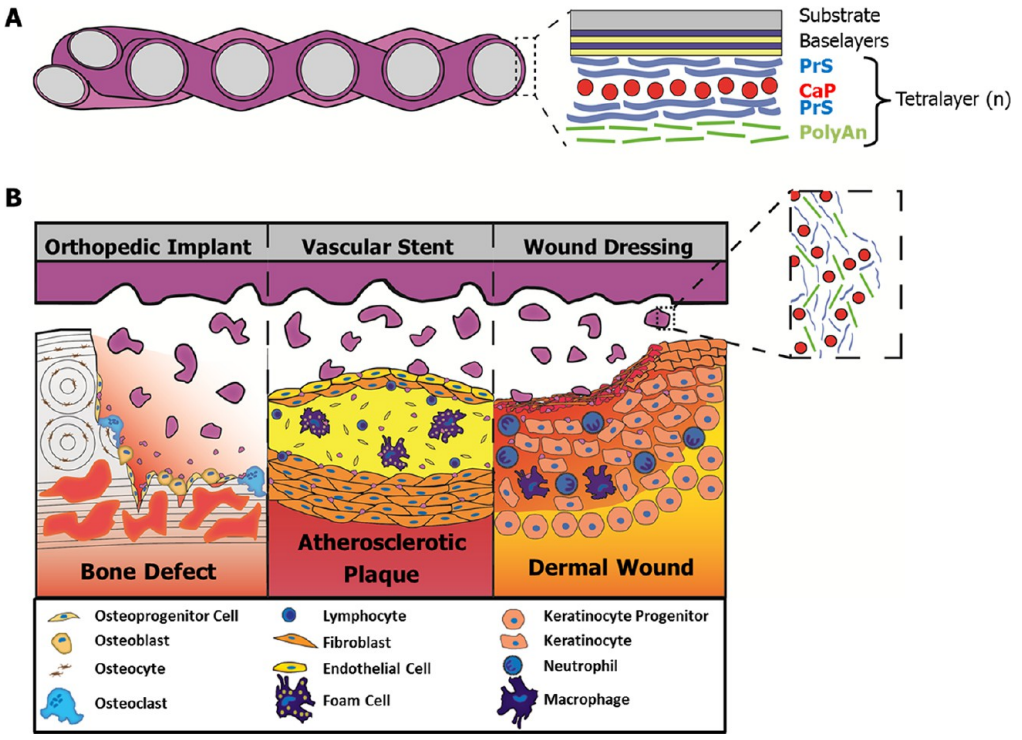

Figure 1. Layer-by-layer coating of Tegaderm and potential applications for localized delivery of siRNA. (A) Schematic representation of LbL film coated Tegaderm. Shown in the zoomed-in portion is a depiction of the Laponite-containing LbL film architecture. (B) Potential application of LbL films releasing siRNA-containing fragments of film into various environments where modulation of cellular responses may provide some therapeutic benefit. Inset illustrates an idealized set of components released from the coating.

with other biologically relevant components[26] may be possible.

Herein we describe the development of an LbL nanolayered coating for the delivery of siRNA that is capable of sustaining significant knockdown in multiple cell lines for more than one week *in vitro*. This film requires no externally delivered transfection vectors such as lipofectamine or mechanical transfection techniques (*e.g.*, electroporation) to achieve these results. The coating was applied to a commercially available woven nylon bandage for testing and showed minimal impact on the viability of cells exposed to it. By tuning the film architecture and the number of layers incorporated into the film, the release rate and amount of siRNA released can be controlled in a systematic fashion. A schematic of the application of such an LbL film is presented in Figure 1a, where the coating is shown applied to a generic woven substrate. Figure 1b illustrates a range of potential applications for such a coating in multiple different localized delivery applications.

RESULTS AND DISCUSSION

siRNA Thin Film Assembly. To achieve optimized loading and release characteristics, four LbL film architectures containing siRNA-loaded calcium phosphate nanoparticles were investigated, using materials design strategies that enabled maximal intracellular release. We chose to use CaP nanoparticles, as they are intrinsically negatively charged and have been shown to remain intact after incorporation into LbL assemblies;[43] however, they dissociate upon maturation of the endosome when the pH falls below approximately 6.8−6.6. The dissociation of CaP within the endosome causes osmotic pressure to increase, leading to endosomal rupture and release of the packaged siRNA into the cytosol.[44,45] The films were constructed of different architectures consisting of bilayer or tetralayer combinations of polyelectrolyte materials. Protamine sulfate (PrS), a naturally derived peptide isolated from salmon sperm, was chosen for the polycation for all films in this paper, as it has an isoelectric point around pH 12[46] and has been shown to complex nucleic acids very effectively.[47−49] PrS consists largely of arginine and has been shown to bind DNA and siRNA and protect them from nuclease degradation for multiple days when exposed to serum nucleases.[49,50] We investigated three polyanions to use in combination with the CaP nanoparticles and PrS in LbL assemblies: (1) low molecular weight (9 kDa) dextran sulfate (DS_L), (2) high molecular weight (500 kDa) dextran sulfate (DS_H), and (3) Laponite silicate clay (Lap).[51] All components are either readily degraded by proteases or other enzymes in the body or are native biomolecules that can be readily resorbed or cleared from the body.

The four film architectures tested in this investigation were (1) (PrS/CaP nanoparticle) bilayers, (2) (PrS/CaP

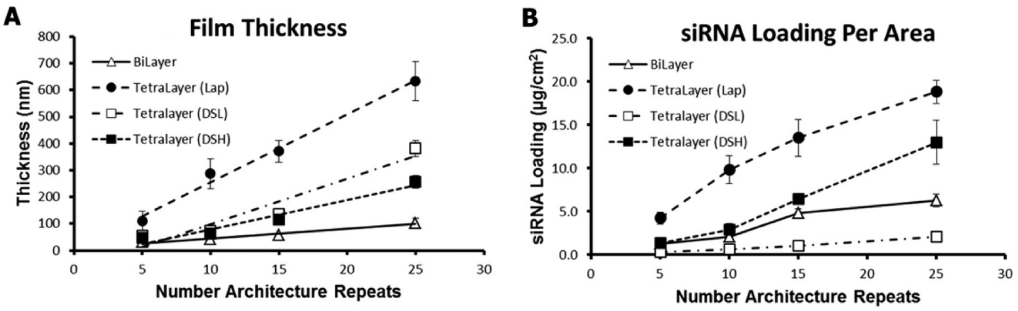

C

	BiLayer	Tetralayer (Lap)	Tetralayer (DS_L)	Tetralayer (DS_H)
Loading Density (μg/mm³)	304 ± 65	149 ± 20	28 ± 7	252 ± 55
Loading Efficiency	0.25 ± 0.03	0.76 ± 0.05	0.08 ± 0.02	0.52 ± 0.10

Figure 2. LbL film growth and siRNA incorporation. (A) Plot of film thickness *versus* the number of film architecture repeats for all four film architectures deposited on flat silicon substrates. The data points represent average measurements taken by both profilometry and elipsometry; error bars represent the 95% confidence interval. (B) Plot of total siRNA loading per film area of all four tested films measured using the Oligreen dsDNA assay of fully degraded samples. (C) Loading density of siRNA with the formed films (μg/mm^3) and the efficiency of siRNA incorporation for film architectures tested at 25 architecture repeats.

nanoparticle/PrS/DS_L) tetralayers, (3) (PrS/CaP nanoparticle/PrS/DS_H) tetralayers, and (4) (PrS/CaP nanoparticle/PrS/Lap) tetralayers. These four different films gave very different results in their respective rates of film growth, siRNA incorporation, and the level of knockdown observed.

CaP nanoparticles were analyzed using a ZetaPALS dynamic light scattering and zeta potential analyzer before and after film construction to evaluate any change in particle characteristics during the film-building process. Prior to film construction the average nanoparticle diameter as measured using dynamic light scattering was approximately 217 nm and the particles had a negative zeta potential of nearly −30 mV. After the generation of the LbL multilayer film (25 bi- or tetralayers), the particle size of the remaining CaP particles in solution was 199 nm and the particles exhibited a similar zeta potential to nanoparticles prior to dipping (−28 mV), indicating little aggregation or dissociation of the CaP siRNA nanoparticles in the disperse phase during film assembly.

Film growth was measured using both profilometry and ellipsometry on films built on silicon substrates.[31,52] The growth curve for each architecture is plotted in Figure 2A. The thinnest film, (PrS/CaP), grew linearly (as plotted R^2 = 0.97) with an average growth rate of approximately 4 nm per layer, reaching 103 ± 18.5 nm after 25 layers. Even after 25 layers this film did not approach a thickness equal to the average diameter of the particles being incorporated, which suggests that much less than a complete monolayer of coverage was obtained during assembly. It is possible that the CaP nanoparticles are disrupted or broken up into smaller nanoparticles during the stresses and capillary forces introduced in electrostatic adsorption to the surface. As free siRNA is also present in solution with the CaP nanoparticles, we also anticipate that both free siRNA and CaP nanoparticles adsorb to the surface. AFM imaging of the surface showed many small particle-sized features that became denser with increasing number of bilayers. The roughness of this film was also seen to increase during growth from approximately 9.6 nm at 5 bilayers to 16.6 nm at 25 bilayers.

The (PrS/CaP/PrS/DS_L) film growth was not truly linear over the 25 layers investigated (as suggested by the plotted R^2 = 0.91 for a linear fit). For the first 15 layers the film grew at approximately 6.8 nm per layer, which increased significantly to nearly 25 nm per layer between layers 15 to 25. Although it is unclear from the growth rate data alone, this kind of increase in film thickness is a characteristic of interdiffusion taking place during film construction.[35,53] After 25 tetralayers, the (PrS/CaP/PrS/DS_L) was the second thickest film tested at 380 ± 30.2 nm and had a surface roughness of approximately 35 nm. Both the Lap- and DS_H-containing films exhibited near linear growth over the 25 architecture repeats (as plotted for R^2 = 0.98, and 0.95, respectively). The (PrS/CaP/PrS/DS_H) grew by nearly 10.5 nm per tetralayer and reached a thickness of 257 ± 24.5 nm at 25 tetralayers, while the (PrS/CaP/PrS/Lap) film grew by approximately 31 nm per layer, reaching 633 ±72 nm at 25 layers. The roughness of these two films was similar (DS_H = 18.3 nm, Lap = 21.6 nm) after 25 layers.

The amount of siRNA incorporated per coated area within the different film architectures varied significantly with the choice of polyanion (Figure 2B).

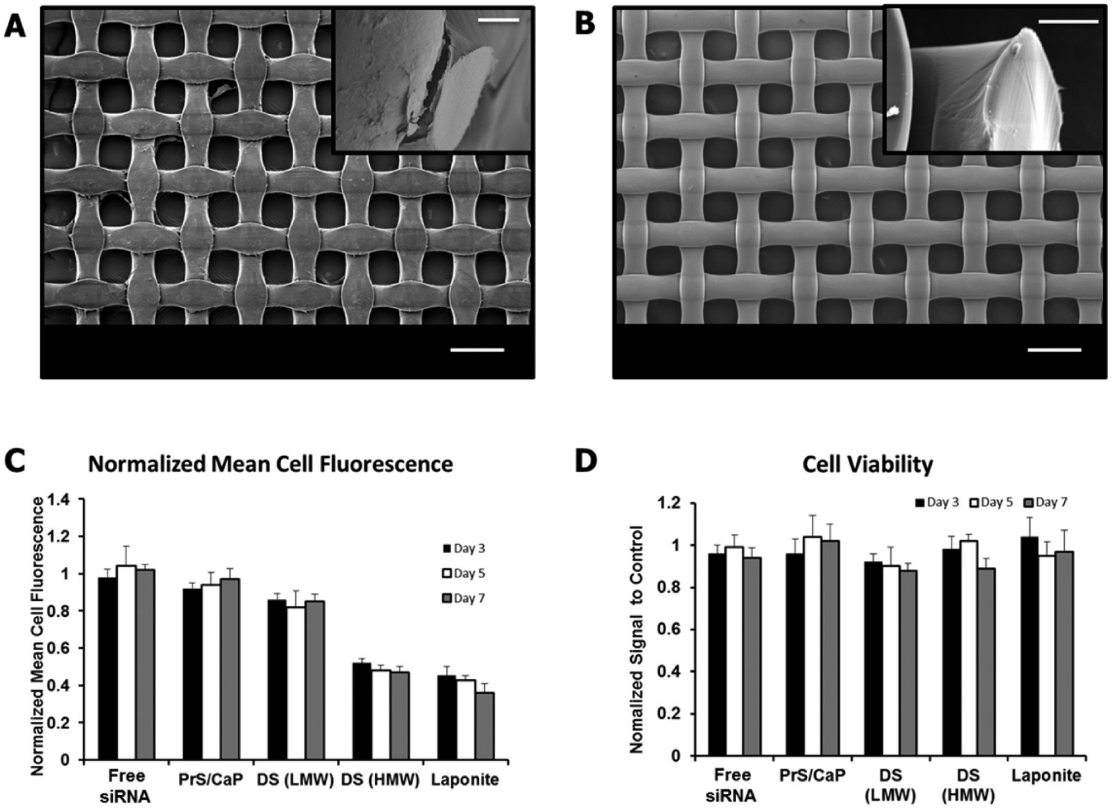

Figure 3. *In vitro* **characterization of LbL films. (A) SEM image showing the regular woven pattern of Laponite-containing film coated on Tegaderm used for *in vitro* testing. Scale bar = 100 μm, inset scale bar = 10 μm. (B) SEM of uncoated Tegaderm substrate. Similar scales to those in A. (C) Plot of flow cytometry data for NIH-3T3 cells stably expressing GFP exposed to LbL film coated Tegaderm for 3 (■), 5 (□), and 7 (gray bars) days. Data are shown as relative mean cell fluorescence normalized to cells treated with siControl-containing films of the same architecture. (D) Cell viability of NIH-3T3 cells exposed to LbL film coated Tegaderm as compared to cells exposed to uncoated Tegaderm, measured using AlamarBlue metabolic assay.**

After 25 layers the (PrS/CaP/PrS/DS_L) film had incorporated the least amount of siRNA, only $2.1 \pm 0.6\,\mu g/cm^2$, while the (PrS/CaP/PrS/Lap) film contained nearly 10 times that amount ($18.9 \pm 1.4\,\mu g/cm^2$). It is interesting to note that increased film thickness did not correlate with increased siRNA loading, as the DS_L-containing film was nearly 1.5 times thicker than the DS_H film at 25 tetralayers and yet held less than one-sixth the amount of siRNA ($12.9 \pm 2.6\,\mu g/cm^2$). The (PrS/CaP) film incorporated $6.3 \pm 0.7\,\mu g/cm^2$ after 25 layers, approximately one-third as much as the Lap-containing tetralayer film; however it was one-sixth as thick. The average siRNA density for each film after 25 architecture repeats is shown in Figure 2C along with the efficiency of siRNA incorporation from the dipping baths for each film.

Each of the four films was built on a nondegradable inert substrate that could be placed in close contact with cells to function as a reservoir from which the films would degrade and release siRNA. We chose to use a woven nylon bandage (Tegaderm) for this substrate. Tegaderm is commonly used in medical practice as a contact layer on top of wounds to reduce tissue infiltration into and unwanted adhesion to the dressing. The structure of the fabric is highly uniform, consisting of woven fibers of approximately 70 μm in diameter, which form pores within the weave of nearly 0.01 mm^2 (Figure 3B). Coating the substrate with LbL film did not disturb these features, as can be seen by SEM in Figure 3A. The inset images are higher magnification views at the edge of the substrate where it has been cut.

Films were created using both siRNA specific for GFP and a control sequence of siRNA that is known to not target any mRNA sequence (siControl). Knockdown of GFP was followed for one week *in vitro*. Film-coated substrates were placed into culture with GFP-expressing NIH-3T3 cells in 48-well plates. All experiments were carried out in 5% FBS-supplemented media as described in the Methods and Materials section of this paper. Media was exchanged from the wells every two days. Relative mean cell fluorescence of the cell populations treated with each of the different film architectures on days 3, 5, and 7 can be seen in Figure 3C. It has been demonstrated that free siRNA does not transfect cells effectively to significantly reduce gene expression. To test that our siRNA sequence behaves similarly, we added 100 pmol of GFP-siRNA in 50 μL of PBS to cells on day 0 and followed mean cell fluorescence over one week. We saw no significant change in

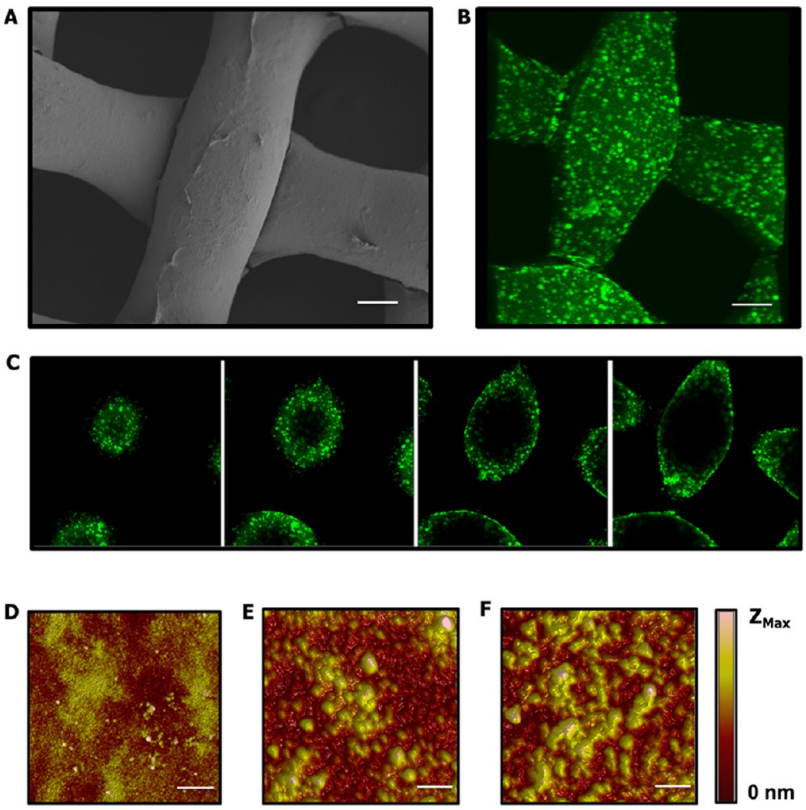

Figure 4. Characterization of Laponite-containing LbL film coating on a Tegaderm substrate. (A) SEM imaging of film-coated substrate; scale bar = 25 μm. (B) Three-dimensional projection of fluorescent confocal imaging of film-coated substrate using AlexaFluor 488-labeled siRNA. Scale bar = 25 μm. (C) Selected confocal images used to generate projected image. Images were selected at 8 μm steps to show the conformal nature of the film coating. (D–F) Atomic force micrographs at 5, 15, and 25 architecture repeats, respectively; Z_{max} = 57 nm (D), 138 nm (E), and 182 nm (F); scale bar = 5 μm.

fluorescence or in cell viability for cells treated with free siRNA.

The expression of GFP was most reduced in cells exposed to the (PrS/CaP/PrS/Lap) film architecture. On day 3, cells exposed to this film had a 55% reduction in mean cell fluorescence, which increased to 58% by day 5 and finally to a 64% reduction by day 7 compared to cells treated with the siControl-containing film. The dextran sulfate-containing films achieved very different levels of knockdown. The (PrS/CaP/PrS/DS_L) film reached a maximum reduction in mean cell fluorescence of approximately 18% on day 5, which decreased slightly by day 7 to only 14%. The (PrS/CaP/PrS/DS_H) film on the other hand achieved nearly a 48% reduction in mean cell fluorescence on day 3, which had increased to a 53% reduction by day 7. The (PrS/CaP) bilayer film showed no measurable reduction in GFP expression over the one-week period *in vitro*. Further investigation showed that this film did not degrade or breakdown to release its contents significantly over the test period.

The impact of each film on cell viability was quantified using the AlamarBlue assay. The viability of cells exposed to film-coated substrates was normalized to cells exposed to uncoated substrates. These results can be seen in Figure 3D. Cells proliferated rapidly under all testing conditions, growing to near confluence by day 5. Exposure of cells to 100 pmol of free siRNA did not impact cell viability significantly. None of the films tested exhibited significant cytotoxicity at any time over the one-week test period.

siRNA Film Characterization. Of the four films tested, the (PrS/CaP/PrS/Lap) film showed the greatest reduction in GFP expression, had the least impact on cell viability, and incorporated the most siRNA per area. For these reasons this film was determined to be the best performing film and was chosen to be the focus of further investigation. SEM imaging of the film-coated substrate showed near uniform coating with some bridges of film appearing to connect the woven fibers (Figure 4A). Incorporation of siRNA was similarly uniform over the coated substrate; as seen in confocal imaging using a fluorescently labeled siRNA in Figure 4B, sections used to render the projection highlight the uniform and continuous nature of the coating of the fibers (Figure 4C). The sections shown are at 8 μm steps, starting near the apex of a fiber, moving through the fiber until reaching the center.

Fluorescent imaging showed punctate localizations of signal within the film coating (Figure 4B). To investigate these formations, the same film was built on silicon substrates and characterized by atomic force

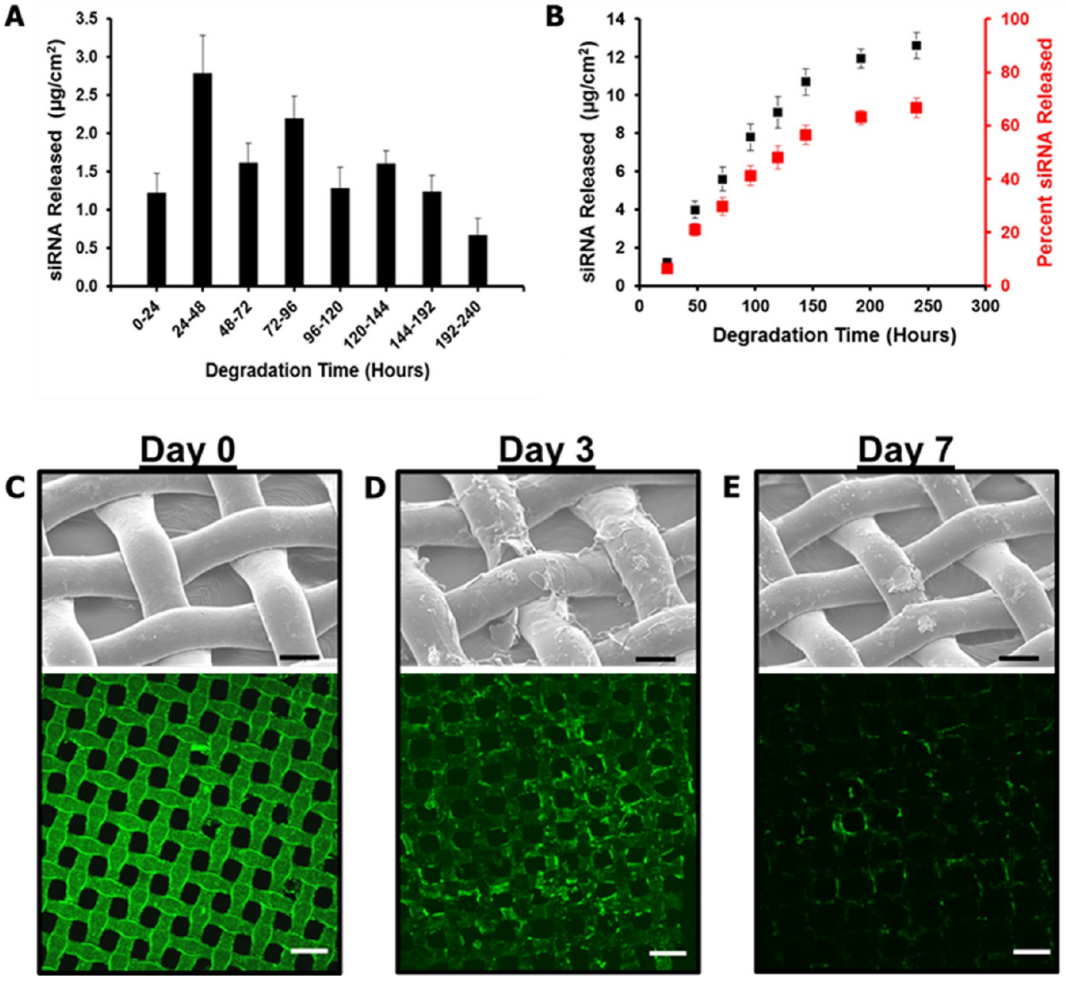

Figure 5. LbL film degradation and release of siRNA. (A) Plot of siRNA release measured daily (days 1−6) or bidaily (days 7−10). Release measured during degradation of FITC-labeled siRNA-containing film in cell-conditioned media. (B) Cumulative release of siRNA over the 10-day period tested. (C−E) Side-by-side comparison of SEM and confocal imaging showing the breakdown of the film on day 0 (C), day 3 (D), and day 7 (E), in cell-conditioned media. SEM scale bar = 50 μm; confocal scale bar = 100 μm.

microscopy (AFM). Figure 4D−F show the surface topography as measured by AFM at 5, 15, and 25 architecture repeats on the surface. Large (approximately 3−5 μm in diameter) features began to appear on the surface of the film at 15 tetralayers. Dynamic light scattering measurements of the solutions used to construct the film showed no particulate in excess of 300 nm in diameter. This suggests that these aggregations are likely formed on the surface during film growth and do not represent the incorporation of pre-existing particle aggregates from solution.

Degradation and Sustained Release Profiles of LbL siRNA in Cell Media. Release of siRNA from the film was followed in cell-conditioned media at 37 °C for 10 days using fluorescently labeled siRNA. The release profile can be seen in Figure 5A and B. Over the first six days of degradation, the film released siRNA at an average rate of 1.8 μg/cm^2 per day. This rate dropped to approximately 0.5 μg/cm^2 per day after day 6 until the end of the study period. The cumulative release of siRNA for the 10 days was 12.7 μg/cm^2. Estimated concentrations of siRNA that cells exposed to this film are in are shown in Supporting Information Figure S2. The total amount of siRNA incorporated within this film was shown to be nearly 19 μg/cm^2, meaning that approximately two-thirds of the siRNA incorporated was released over the 10-day test period. No further release of siRNA from the film was observed after 10 days.

The breakdown and release of the film from the substrate was monitored optically by SEM and fluorescent imaging. A sample taken prior to dissociation of the film is shown in Figure 5C. The unexposed film coats the substrate with few surface defects, and fluorescent imaging shows uniform covering of the substrate with only a few areas of increased fluorescent signal. Samples of the film were taken on day 3 and day 7 to inspect the film that remained attached to the substrate. Images at three days show that the film had swollen noticeably and that the distribution of fluorescence along the substrate surface had become less uniform. SEM images show large surface defects in the coating with significant portions of the film loosely

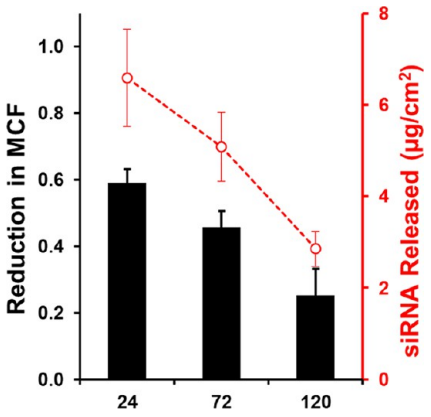

Figure 6. Continued function of siRNA released from LbL films assessed over a one-week period *in vitro*. Films introduced to cells after degradation in cell-conditioned media for up to five days (120 h) prior to introduction to cells were still able to affect knockdown of GFP in NIH-3T3 cells. Total siRNA released during the period tested is shown in red.

bound to the substrate (Figure 5D). By day 7 most of the film had been released from the substrate with only a few large pieces of film remaining attached to the surface. The fluorescent images of the film at this point also show that most of the labeled siRNA contained within the film had been released (Figure 5E).

Demonstration of Maintained siRNA Bioactivity. Degradation and release studies showed that siRNA was released from the LbL film for up to 10 days *in vitro*. As siRNA is known to undergo rapid nuclease degradation when unprotected,[1,2] it was important to ensure that the siRNA released at later time points was still bioactive. To investigate this, films were released for 24, 72, or 120 h in cell-conditioned media prior to introduction to GFP-expressing NIH-3T3 cells. Cells were then exposed to these partially released films for 72 h, and mean cell fluorescence was measured using flow cytometry one day later (Figure 6). All films tested reduced GFP expression relative to control films. The extent to which the films reduced mean cell fluorescence was comparable to the estimated siRNA release under the test conditions (Figure 6). A slight reduction in function could also be due to degradation of the siRNA released or changes in the way that the siRNA is complexed when it is released from the film at later periods. On the basis of these results, it appears that the siRNA activity is relatively unchanged after incorporation in the film, even after a period of several days' release.

Cellular Uptake of siRNA. The uptake of siRNA released from the degrading film was followed in NIH-3T3 cells using a fluorescently labeled siRNA over a one-week period. Figure 7 shows images of 3T3 cells after being exposed to the degrading film for 3, 5, and 7 days, respectively. At day 3 the fluorescent signal within the cells was largely localized to punctate spots. By day 5 and 7 cells were more diffusely fluorescent, although they still contained many punctate localizations of fluorescent signal. The diffuse fluorescence suggests

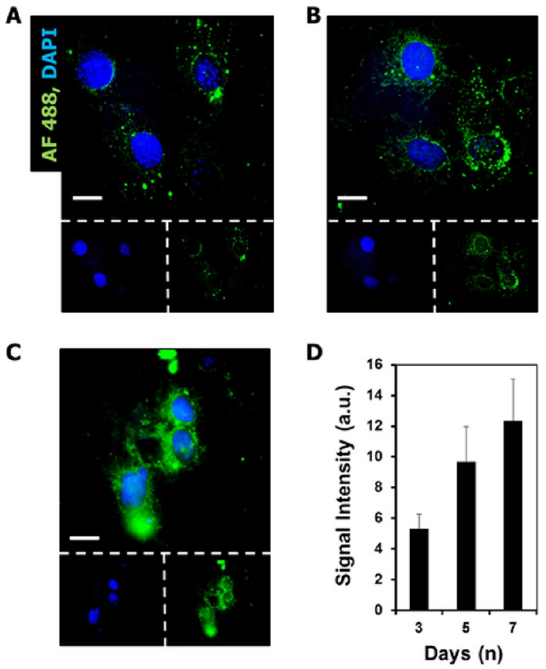

Figure 7. siRNA released from LbL assembly continues to transfect cells and remains active over one-week period *in vitro*. (A–C) Uptake of FITC-labeled siRNA by NIH-3T3 cells at 3 (A), 5 (B), and 7 (C) days' exposure to LbL films containing labeled siRNA. Cells were seen to become more diffusely fluorescent over the one-week period. Scale bar = 10 μm. (D) Average fluorescent intensity of cells.

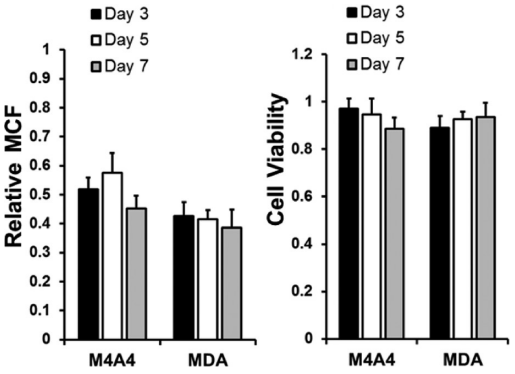

Figure 8. Knockdown of GFP characterized in two separate cancer cell lines. (A) Flow cytometry measurement of mean cell fluorescence of either MDA or M4A4 cells that constitutively express GFP exposed to GFP-siRNA-containing LbL films followed over a one-week period. Data shown are normalized to mean cell fluorescence of cells exposed to siControl-containing film of the same architecture. (B) Viability of cells exposed to coated Tegaderm substrate normalized to cells exposed to uncoated substrates. Viability was measured by the AlamarBlue metabolic assay.

that the siRNA is escaping the more localized environment of endosomal compartments and diffusing into the cytosol.

Extension to Knockdown in MDA-MB-435 and M4A4 Cells. To this point we performed all knockdown experiments using NIH-3T3s as a representative cell type. To evaluate the effectiveness of this film in achieving knockdown in more cell types, we chose to investigate two

commonly used cancer cell lines that were made to constitutively express GFP, MDA-MB-435, and M4A4. Similar to testing with 3T3 cells, knockdown of GFP was seen by day 3 in both cell types and was maintained for the entire one-week study (Figure 8A). Cell viability was seen to be reduced (Figure 8B) in the M4A4 cells over the one-week period, although it remained relatively high (~90%) compared to that of cells treated with uncoated controls. These results suggest that delivery of siRNA from this film can transfect multiple cell types and provide interesting capabilities for this modular platform in future use.

CONCLUSIONS

The nanolayered siRNA dressings presented in this work demonstrate a truly effective method for the incorporation and localized delivery of siRNA for sustained time periods; the knockdown period and efficacy surpass many other surface-based localized release systems for RNAi. When coated with the film developed here, plain nylon bandages achieved and maintained significant gene knockdown in multiple cell lines for one week *in vitro* without externally applied transfection agents. The films are only a few hundred nanometers in thickness and coat the dressings uniformly, leaving the structure of the bandage unaffected. In total we detailed four distinct siRNA-delivering LbL film architectures and evaluated these systems to isolate the best performing system for a more focused investigation. The materials used in creating the films were all biocompatible and FDA approved, and all process steps were performed under mild aqueous conditions that enabled the maintenance of RNAi activity during assembly of the film. Further, the knockdown of GFP was seen in multiple cell lines including NIH-3T3, MDA-MB-435, and M4A4 cells with similar reductions in GFP expression and with high cell viability. This approach demonstrates the capability of the LbL approach to generate high-density RNAi release systems that can release directly to cells without toxicity and with no mechanical or chemical assistance. We show the nature of release and significant gene knockdown over a sustained period of a week, while observing direct uptake of the siRNA by cells and effective release to the cytosol. Finally, we show the impact that different multilayer compositions have on drug delivery characteristics, independent of film thickness or drug loading.

The ability to deliver siRNA locally in a controlled and sustained manner is a promising tool in many areas where modulation of local cellular responses could provide benefit. The capability to load siRNA into an ultrathin polymer coating for safe and effective delivery of siRNA over an extended period of time provides a significant advance in the existing capabilities of RNA interference. The film described in this work has great potential in many applications ranging from coatings for medical implants and tissue engineering constructs to uses in molecular biology and basic research.

METHODS AND MATERIALS

Materials. siRNA for GFP and siControl were received as a gift from Sanofi-Aventis. AlexaFluor 488-labeled siRNA was purchased from Qiagen (Valencia, CA, USA). Linear poly(ethyleneimine) (LPEI, MW = 25 kDa) and dextran sulfate (DS, MW = 500 kDa or 9 kDa) were purchased from Polysciences (Warrington, PA, USA). Phosphate-buffered saline solution (PBS, 10×), Advanced-MEM, fetal bovine serum, antibiotic−antimycotic solution, and 200 mM L-glutamine solution were purchased from Invitrogen (Carlsbad, CA, USA). GFP-expressing NIH-3T3 cells were purchased from Cell Biolabs (San Diego, CA, USA). NIH-3T3, MDA-MB-435, and M4A4 cells were purchased from ATCC (Manassas, VA, USA). Tegaderm was purchased from Cardinal Health (Newark, NJ, USA).

Formation of siRNA-Loaded Calcium Phosphate Nanoparticles. Calcium phosphate nanoparticles containing siRNA were synthesized by rapid precipitation of $CaCl_2$ and NH_3PO_4 in the presence of siRNA. NH_3PO_4 (3.74 mM) and $CaCl_2$ (6.25 mM) working solutions were prepared in nuclease-free water pH 8.5 and filtered using a 0.2 μm syringe filter. To prepare 3 mL of CaP nanoparticles, a dipping solution containing 20 μg/mL siRNA and 200 μL of NH_3PO_4 was added to 60 μg of siRNA in 100 μL of nuclease-free water. Then 200 μL of the $CaCl_2$ solution was added with vigorous mixing. After approximately 30 s 2.5 mL of pH 8.5 nuclease-free water was then added to dilute the particles to the dipping concentration. The diameter and zeta potential of the formed nanoparticle were measured both prior to and after film assembly using a ZetaPALS dynamic light scattering and zeta potential analyzer. The CaP siRNA particles were always prepared just prior to LbL film construction.

Fabrication of LbL Films. Film assembly was performed using an HMS series Carl-Zeiss programmable slide stainer. Substrates to be coated were first cleaned sequentially with methanol, ethanol, 2-propanol, and water and then dried under filtered nitrogen. These substrates were plasma cleaned for 5 min on the high RF setting and then immediately placed in a 2 mg/mL solution of LPEI and allowed to adsorb the material for at least 30 min prior to use. After this initial coating, substrates were then placed into specially designed holders for the programmable slide stainer to move between dipping baths. A generic bilayer LbL assembly protocol consists of first dipping the substrate into a polycation solution for some specified time, then moving that substrate through two wash steps, where excess polymer is allowed to desorb from the surface. The washed substrate is then placed in a polyanion solution and allowed to adsorb polymer. After adsorption of the polyanion the substrate is then washed two more times to remove any excess polymer. This process can then be repeated for multiple depositions of the bilayer architecture.

All films were assembled on top of 10 base layers of (LPEI/DS) to ensure a conformal charged coating of the substrate for siRNA film deposition. Assembly of base layers was carried out in 100 mM sodium acetate solution at pH 5.0. All solutions were filtered using a 0.2 μm membrane syringe filter prior to use. Polymer solutions used were prepared at a 2 mg/mL concentration, and all CaP nanoparticle solutions contained an approximately 20 μg/mL concentration of siRNA. Polymer deposition steps were done for 10 min, and CaP nanoparticle deposition steps were done for 45 min. All deposition steps were followed with two 1 min washes in pH-adjusted nuclease-free water. All solutions for siRNA-containing films were prepared in pH 9.0 nuclease-free water.

Film Thickness and Surface Characterization. The thickness of the LbL films was assessed for films assembled on silicon and glass substrates using both spectroscopic ellipsometry (XLS-100

spectroscopic ellipsometer, J.A. Woollam Co., Inc.) and profilometry (Dektak 150 profilometer). Ellipsometric measurements were performed on LbL films assembled on silicon substrates. Films were dried under filtered nitrogen prior to measurement. Measurements were performed at room temperature with a 70° incidence angle. The acquired spectra were then fit with a Cauchy dispersion model to obtain an estimated thickness for the film. For measurement of film thickness by profilometry, films were built on either silicon or glass and scored by a razor, then tracked over. Step height from the untouched film to the bottom of the score was measured in six different locations on each sample to obtain an average thickness.

Atomic force microscopy was performed using a Dimension 3100 AFM with a Nanoscope 5 controller (Veeco Metrology) in tapping mode. Film areas of 25 μm by 25 μm were examined for each film after 5, 15, and 25 architecture depositions. Nanoscope Analysis v1.10 software was used to calculate the root mean squared roughness for films.

Quantification of siRNA Loading into the LbL Assembly. Incorporation of siRNA within the LbL film assemblies was quantified after 5, 10, 15, and 25 architecture repeats. To quantify the amount of siRNA within the film, a one square centimeter sample of a film-coated substrate was placed into 500 μL of a 1 M NaCl solution prepared from nuclease-free water. The sample was then subjected to vigorous agitation for 30 min to completely remove the film from the surface. The substrate was then removed from the salt solution, washed with deionized water, and dried under filtered nitrogen. These substrates were evaluated by SEM to check that the entire film had been removed from the surface. Quantification of siRNA was performed using Oligreen dsDNA reagent (Invitrogen) as per the manufacturer's instructions. The degradation solution containing the released film was diluted 1:20 into nuclease-free water to reduce salt concentration to within the tolerance range of the assay. Then 25 μL of degradation sample was added to 100 μL of prepared Oligreen reagent (diluted 1:200 in TE buffer of reagent in kit) in a FluoroBlok (BD) 96-well plate. Samples were then read with a fluorescent plate reader with 490/520 Ex/Em wavelengths. Standards were prepared using similar salt concentrations to that in the diluted degradation samples.

Degradation Studies and Release Characterization. Experiments for the quantification of film degradation were carried out in cell-conditioned media. To assist in the visualization of the degradation of the film, AlexaFluor 488-labeled siRNA was used. Cell-conditioned media was prepared from NIH-3T3 cells grown to confluence. NIH-3T3s were seeded into 24-well plates (50 000 cells/well) and cultured in Advanced-MEM (Invitrogen) media containing 5% FBS, 1% antibiotic–antimycotic solution, and 2 mM L-glutamine. Cells grew to confluence within approximately one day after seeding. Media was removed from wells after 72 h in contact with the cells. This media was filtered using a 0.2 μm syringe filter to remove cellular debris. This filtered media was then placed directly onto the films to be degraded. Degradations were carried out at 37 °C with the entire degradation media exchanged daily. Unlabeled siRNA served as a blank nonfluorescent control. A standard curve of the fluorescently labeled siRNA was used to interpret the concentration of siRNA within the release media. SEM analysis of all samples was done using a JEOL 6700F scanning electron microscope. Confocal imaging of degrading samples was performed on a Zeiss LSM 510 confocal laser scanning microscope.

Characterization of *in Vitro* Knockdown. GFP knockdown was characterized by flow cytometry measurements of mean cell fluorescence in NIH-3T3, MDA-MB-435, and M4A4 cells that constitutively expressed GFP. A total of 5000 cells per well were seeded in a 48-well plate in 600 μL of cell growth media and allowed to incubate for 24 h. Film-coated substrates were cut into 0.5 $\times$ 0.5 cm (0.25 cm^2 total area) squares and placed into the wells with the cells. After 3, 5, or 7 days of exposure to the film-coated substrates cells were trypsinized and mean cell fluorescence was determined by flow cytometry, using a BD FACSCalibur flow cytometer.

Preservation of siRNA Knockdown during Release. Films were created using GFP-specific siRNA. GFP-expressing NIH-3T3s were seeded as previously described. Films were predegraded in cell-conditioned media for 24, 72, or 120 h and then placed in culture with the cells. Cells were exposed to films for 72 h. Mean cell fluorescence was measured using flow cytometry. Films containing negative control siRNA were used for quantification of relative cell fluorescence.

***In Vitro* Transfection with Fluorescently Labeled siRNA.** Transfection of NIH-3T3s was monitored using fluorescently labeled siRNA. Similar to knockdown experiments, films containing the labeled siRNA were built on Tegaderm samples and placed in culture with NIH-3T3 cells grown on coverslips in cell growth media. Cells were exposed to films for up to one week *in vitro* with media being changed every two days. At day 3, 5, and 7 samples were taken for microscope analysis of transfection. Cells were fixed in formalin diluted in PBS and counterstained with DAPI nuclear stain.

Conflict of Interest: The authors declare no competing financial interest.

Supporting Information Available: S1: Confocal imaging of AlexaFluor-488-labeled siRNA containing Laponite film material as released onto NIH-3T3 cells in culture. The images were taken after exposure to the releasing film for 7 days. S2: Estimate of siRNA concentration within cell media released from Laponite-containing tetralayer film during *in vitro* knockdown studies. This material is available free of charge *via* the Internet at http://pubs.acs.org.

Acknowledgment. This research was supported in part by funding and core facilities provided by the U.S. Army Research Office under contract W911NF-07-D-0004 at the MIT Institute of Soldier Nanotechnology and by funding from the Sanofi-Aventis and MIT Center for Biomedical Innovation. This work was also supported by use of core facilities at the Koch Institute for Integrative Cancer Research (supported by the NCI under grant 2P30CA014051-39). We thank the Koch Institute Swanson Biotechnology Center for technical support, specifically the microscopy and flow cytometry cores. The authors wish to dedicate this paper to the memory of Officer Sean Collier, for his caring service to the MIT community and for his sacrifice.

REFERENCES AND NOTES

1. Whitehead, K. A.; Langer, R.; Anderson, D. G. Knocking Down Barriers: Advances in siRNA Delivery. *Nat. Rev. Drug Discovery* **2009**, *8*, 129–138.
2. Gavrilov, K.; Saltzman, W. M. Therapeutic SiRNA: Principles, Challenges, and Strategies. *Yale J. Biol. Med.* **2012**, *85*, 187–200.
3. Vaishnaw, A. K.; Gollob, J.; Gamba-Vitalo, C.; Hutabarat, R.; Sah, D.; Meyers, R.; de Fougerolles, T.; Maraganore, J. A Status Report on RNAi Therapeutics. *Silence* **2010**, *1*, 14.
4. Guo, P.; Coban, O.; Snead, N. M.; Trebley, J.; Hoeprich, S.; Guo, S.; Shu, Y. Engineering RNA for Targeted SiRNA Delivery and Medical Application. *Adv. Drug Delivery Rev.* **2010**, *62*, 650–666.
5. Ghildiyal, M.; Zamore, P. D. Small Silencing RNAs: An Expanding Universe. *Nat. Rev. Genet.* **2009**, *10*, 94–108.
6. Burnett, J. C.; Rossi, J. J. RNA-Based Therapeutics: Current Progress and Future Prospects. *Chem. Biol. (Oxford, U. K.)* **2012**, *19*, 60–71.
7. Ballarín-González, B.; Howard, K. A. Polycation-Based Nanoparticle Delivery of RNAi Therapeutics: Adverse Effects and Solutions. *Adv. Drug Delivery Rev.* **2012**, *64*, 1717–1729.
8. Wu, Z. W.; Chien, C. T.; Liu, C. Y.; Yan, J. Y.; Lin, S. Y. Recent Progress in Copolymer-Mediated SiRNA Delivery. *J. Drug Targeting* **2012**, *20*, 551–560.
9. Liu, J.; Guo, S.; Cinier, M.; Shlyakhtenko, L. S.; Shu, Y.; Chen, C.; Shen, G.; Guo, P. Fabrication of Stable and RNase-Resistant RNA Nanoparticles Active in Gearing the Nanomotors for Viral DNA Packaging. *ACS Nano* **2011**, *5*, 237–246.
10. Juliano, R.; Bauman, J.; Kang, H.; Ming, X. Biological Barriers to Therapy with Antisense and SiRNA Oligonucleotides. *Mol. Pharmacol.* **2009**, *6*, 686–695.

11. McNamara, J. O., 2nd; Andrechek, E. R.; Wang, Y.; Viles, K. D.; Rempel, R. E.; Gilboa, E.; Sullenger, B. A.; Giangrande, P. H. Cell Type-Specific Delivery of SiRNAs with Aptamer-SiRNA Chimeras. *Nat. Biotechnol.* **2006**, *24*, 1005–1015.
12. Takeshita, F.; Minakuchi, Y.; Nagahara, S.; Honma, K.; Sasaki, H.; Hirai, K.; Teratani, T.; Namatame, N.; Yamamoto, Y.; Hanai, K.; *et al*. Efficient Delivery of Small Interfering RNA to Bone-Metastatic Tumors by Using Atelocollagen *in Vivo*. *Proc. Natl. Acad. Sci. U.S.A.* **2005**, *102*, 12177–12182.
13. Lorenz, C.; Hadwiger, P.; John, M.; Vornlocher, H. P.; Unverzagt, C. Steroid and Lipid Conjugates of SiRNAs to Enhance Cellular Uptake and Gene Silencing in Liver Cells. *Bioorg. Med. Chem. Lett.* **2004**, *14*, 4975–4977.
14. Schiffelers, R. M.; Ansari, A.; Xu, J.; Zhou, Q.; Tang, Q.; Storm, G.; Molema, G.; Lu, P. Y.; Scaria, P. V.; Woodle, M. C. Cancer SiRNA Therapy by Tumor Selective Delivery with Ligand-Targeted Sterically Stabilized Nanoparticle. *Nucleic Acids Res.* **2004**, *32*, e149.
15. Shu, Y.; Cinier, M.; Shu, D.; Guo, P. Assembly of Multifunctional phi29 pRNA Nanoparticles for Specific Delivery of SiRNA and Other Therapeutics to Targeted Cells. *Methods (Amsterdam, Neth.)* **2011**, *54*, 204–214.
16. Alam, M. R.; Ming, X.; Fisher, M.; Lackey, J. G.; Rajeev, K. G.; Manoharan, M.; Juliano, R. L. Multivalent Cyclic RGD Conjugates for Targeted Delivery of Small Interfering RNA. *Bioconjugate Chem.* **2011**, *22*, 1673–1681.
17. Xiao, Z.; Farokhzad, O. C. Aptamer-Functionalized Nanoparticles for Medical Applications: Challenges and Opportunities. *ACS Nano* **2012**, *6*, 3670–3676.
18. Che, H.-L.; Bae, I.-H.; Lim, K. S.; Song, I. T.; Lee, H.; Muthiah, M.; Namgung, R.; Kim, W. J.; Kim, D.-G.; Ahn, Y.; *et al*. Suppression of Post-Angioplasty Restenosis with an Akt1 SiRNA-Embedded Coronary Stent in a Rabbit Model. *Biomaterials* **2012**, *33*, 8548–8556.
19. Li, J. M.; Newburger, P. E.; Gounis, M. J.; Dargon, P.; Zhang, X.; Messina, L. M. Local Arterial Nanoparticle Delivery of SiRNA for NOX2 Knockdown to Prevent Restenosis in an Atherosclerotic Rat Model. *Gene Ther.* **2010**, *17*, 1279–1287.
20. Dimitrova, M.; Affolter, C.; Meyer, F.; Nguyen, I.; Richard, D. G.; Schuster, C.; Bartenschlager, R.; Voegel, J. C.; Ogier, J.; Baumert, T. F. Sustained Delivery of SiRNAs Targeting Viral Infection by Cell-Degradable Multilayered Polyelectrolyte Films. *Proc. Natl. Acad. Sci. U.S.A.* **2008**, *105*, 16320–16325.
21. Nelson, C. E.; Gupta, M. K.; Adolph, E. J.; Shannon, J. M.; Guelcher, S. A.; Duvall, C. L. Sustained Local Delivery of SiRNA from an Injectable Scaffold. *Biomaterials* **2012**, *33*, 1154–1161.
22. Nguyen, K.; Dang, P. N.; Alsberg, E. Functionalized, Biodegradable Hydrogels for Control over Sustained and Localized SiRNA Delivery to Incorporated and Surrounding Cells. *Acta Biomater.* **2013**, *9*, 4487–4495.
23. Rujitanaroj, P. O.; Wang, Y. C.; Wang, J.; Chew, S. Y. Nanofiber-Mediated Controlled Release of SiRNA Complexes for Long Term Gene-Silencing Applications. *Biomaterials* **2011**, *32*, 5915–5923.
24. Katz, M. G.; Fargnoli, A. S.; Pritchette, L. A.; Bridges, C. R. Gene Delivery Technologies for Cardiac Applications. *Gene Ther.* **2012**, *19*, 659–669.
25. Wolinsky, J. B.; Colson, Y. L.; Grinstaff, M. W. Local Drug Delivery Strategies for Cancer Treatment: Gels, Nanoparticles, Polymeric Films, Rods, and Wafers. *J. Controlled Release* **2012**, *159*, 14–26.
26. Manaka, T.; Suzuki, A.; Takayama, K.; Imai, Y.; Nakamura, H.; Takaoka, K. Local Delivery of SiRNA Using a Biodegradable Polymer Application to Enhance BMP-Induced Bone Formation. *Biomaterials* **2011**, *32*, 9642–9648.
27. Rujitanaroj, P.-o.; Jao, B.; Yang, J.; Wang, F.; Anderson, J. M.; Wang, J.; Chew, S. Y. Controlling Fibrous Capsule Formation through Long-Term Down-Regulation of Collagen Type I (COL1A1) Expression by Nanofiber-Mediated SiRNA Gene Silencing. *Acta Biomater.* **2012**, *9*, 4513–4524.
28. Chen, M. Chitosan/SiRNA Nanoparticles Encapsulated in PLGA Nanofibers for siRNA Delivery. *ACS Nano* **2012**, *6*, 4835–4844.
29. Hammond, P. T. Building Biomedical Materials Layer-by-Layer. *Mater. Today* **2012**, *15*, 196–206.
30. Jewell, C. M. Multilayered Polyelectrolyte Assemblies as Platforms for the Delivery of DNA and Other Nucleic Acid-Based Therapeutics. *Adv. Drug Delivery Rev.* **2008**, *60*, 979–999.
31. Shah, N. J.; Hong, J.; Hyder, M. N.; Hammond, P. T. Osteophilic Multilayer Coatings for Accelerated Bone Tissue Growth. *Adv. Mater. (Weinheim, Ger.)* **2012**, *24*, 1445–1450.
32. Shukla, A.; Fang, J. C.; Puranam, S.; Jensen, F. R.; Hammond, P. T. Hemostatic Multilayer Coatings. *Adv. Mater. (Weinheim, Ger.)* **2012**, *24*, 492–496.
33. Detzel, C. J.; Larkin, A. L.; Rajagopalan, P. Polyelectrolyte Multilayers in Tissue Engineering. *Tissue Eng., Part B* **2011**, *17*, 101–113.
34. Zelikin, A. N. Drug Releasing Polymer Thin Films: New Era of Surface-Mediated Drug Delivery. *ACS Nano* **2010**, *4*, 2494–2509.
35. Shukla, A.; Avadhany, S. N.; Fang, J. C.; Hammond, P. T. Tunable Vancomycin Releasing Surfaces for Biomedical Applications. *Small* **2010**, *6*, 2392–2404.
36. Shah, N. J.; Hong, J.; Hyder, M. N.; Hammond, P. T. Osteophilic Multilayer Coatings for Accelerated Bone Tissue Growth. *Adv. Mater. (Weinheim, Ger.)* **2012**, *24*, 1445–1450.
37. Zhao, Z.; Qi, Y.; Wei, M.; Zhang, F.; Xu, S. Layer-by-Layer Assembly and Morphological Characterizations of DNA/Layered Double Hydroxide Thin Films. *Mater. Lett.* **2012**, *78*, 62–65.
38. Aytar, B. S.; Prausnitz, M. R.; Lynn, D. M. Rapid Release of Plasmid DNA from Surfaces Coated with Polyelectrolyte Multilayers Promoted by the Application of Electrochemical Potentials. *ACS Appl. Mater. Interfaces* **2012**, *4*, 2726–2734.
39. Liu, S.; Liu, T.; Chen, J.; Maitz, M.; Chen, C.; Huang, N. Influence of a Layer-by-Layer-Assembled Multilayer of anti-CD34 Antibody, Vascular Endothelial Growth Factor, and Heparin on the Endothelialization and Anticoagulation of Titanium Surface. *J. Biomed. Mater. Res., Part A* **2012**, *101*, 1144–1157.
40. Hillberg, A. L.; Tabrizian, M. Biorecognition through Layer-by-Layer Polyelectrolyte Assembly: In-Situ Hybridization on Living Cells. *Biomacromolecules* **2006**, *7*, 2742–2750.
41. Wood, K. C.; Chuang, H. F.; Batten, R. D.; Lynn, D. M.; Hammond, P. T. Controlling Interlayer Diffusion to Achieve Sustained, Multiagent Delivery from Layer-by-Layer Thin Films. *Proc. Natl. Acad. Sci. U.S.A.* **2006**, *103*, 10207–10212.
42. Hong, J. Graphene Multilayers as Gates for Multi-Week Sequential Release of Proteins from Surfaces. *ACS Nano* **2012**, *6*, 81–88.
43. Zhang, X.; Kovtun, A.; Mendoza-Palomares, C.; Oulad-Abdelghani, M.; Fioretti, F.; Rinckenbach, S.; Mainard, D.; Epple, M.; Benkirane-Jessel, N. SiRNA-Loaded Multi-Shell Nanoparticles Incorporated into a Multilayered Film as a Reservoir for Gene Silencing. *Biomaterials* **2010**, *31*, 6013–6018.
44. Sokolova, V.; Epple, M. Inorganic Nanoparticles as Carriers of Nucleic Acids into Cells. *Angew. Chem., Int. Ed.* **2008**, *47*, 1382–1395.
45. Li, J.; Chen, Y. C.; Tseng, Y. C.; Mozumdar, S.; Huang, L. Biodegradable Calcium Phosphate Nanoparticle with Lipid Coating for Systemic siRNA Delivery. *J. Controlled Release* **2010**, *142*, 416–421.
46. Remington, J. P. *Remington, The Science and Practice of Pharmacy*; Mack Pub. Co.: Easton, PA, 1995; p v.
47. Maclachlan, I. siRNAs with Guts. *Nat. Biotechnol.* **2008**, *26*, 403–405.
48. Chen, Y.; Bathula, S. R.; Li, J.; Huang, L. Multifunctional Nanoparticles Delivering Small Interfering RNA and Doxorubicin Overcome Drug Resistance in Cancer. *J. Biol. Chem.* **2010**, *285*, 22639–22650.
49. DeLong, R. K.; Akhtar, U.; Sallee, M.; Parker, B.; Barber, S.; Zhang, J.; Craig, M.; Garrad, R.; Hickey, A. J.; Engstrom, E. Characterization and Performance of Nucleic Acid Nanoparticles Combined with Protamine and Gold. *Biomaterials* **2009**, *30*, 6451–6459.

50. Paris, C.; Moreau, V.; Deglane, G.; Karim, L.; Couturier, B.; Bonnet, M. E.; Kedinger, V.; Messmer, M.; Bolcato-Bellemin, A. L.; Behr, J. P.; *et al*. Conjugating Phosphospermines to siRNAs for Improved Stability in Serum, Intracellular Delivery and RNAi-Mediated Gene Silencing. *Mol. Pharmacol.* **2012**, *9*, 3464–3475.
51. Dawson, J. I.; Kanczler, J. M.; Yang, X. B.; Attard, G. S.; Oreffo, R. O. C. Clay Gels for the Delivery of Regenerative Microenvironments. *Adv. Mater. (Weinheim, Ger.)* **2011**, *23*, 3304–3308.
52. Jourdainne, L.; Arntz, Y.; Senger, B.; Debry, C.; Voegel, J. C.; Schaaf, P.; Lavalle, P. Multiple Strata of Exponentially Growing Polyelectrolyte Multilayer Films. *Macromolecules (Washington, DC, U. S.)* **2007**, *40*, 316–321.
53. Zacharia, N. S.; Modestino, M.; Hammond, P. T. Factors Influencing the Interdiffusion of Weak Polycations in Multilayers. *Macromolecules (Washington, DC, U. S.)* **2007**, *40*, 9523–9528.